

# A Higher-Accuracy van der Waals Density Functional

Kyuho Lee,<sup>1</sup> Éamonn D. Murray,<sup>1</sup> Lingzhu Kong,<sup>1</sup> Bengt I. Lundqvist,<sup>2,3</sup> and David C. Langreth<sup>1</sup>

<sup>1</sup>*Department of Physics and Astronomy, Rutgers University, Piscataway, New Jersey 08854-8019, USA*

<sup>2</sup>*Department of Applied Physics, Chalmers University of Technology, SE - 41296 Göteborg, Sweden*

<sup>3</sup>*Center for Atomic-scale Materials Design, Department of Physics*

*Technical University of Denmark, DK - 2800 Kongens Lyngby, Denmark*

(ΩDated: October 31, 2018)

We propose a second version of the van der Waals density functional (vdW-DF2) of Dion et al. [Phys. Rev. Lett. **92**, 246401 (2004)], employing a more accurate semilocal exchange functional and the use of a large- $N$  asymptote gradient correction in determining the vdW kernel. The predicted binding energy, equilibrium separation, and potential-energy curve shape are close to those of accurate quantum chemical calculations on 22 duplexes. We anticipate the enabling of chemically accurate calculations in sparse materials of importance for condensed-matter, surface, chemical, and biological physics.

The van der Waals (vdW) attraction is a quantum-mechanical phenomenon with charge fluctuations in one part of an atomic system that are electrostatically correlated with charge fluctuations in another. The vdW force at one point thus depends on charge events at another region and is a truly nonlocal correlation effect.

Methods for accurately calculating the vdW interactions in molecules or solids are critical to understanding sparse matter, including bulk solids (*e.g.*, graphite, molecular crystals, and polymers), surface phenomena (*e.g.*, adsorption, water overlayers, and hydrogen storage), and biostructures (*e.g.*, DNA, protein structure, and folding).

The exact density functional contains the vdW forces. Unfortunately, we do not have access to it, but approximate versions are abundant. Commonly, the local-density approximation (LDA) and generalized gradient approximation (GGA) are used with quite some success for dense matter, including hard materials and covalently bound molecules. They depend on the density in local and semilocal ways, respectively, however, and give no account of the fully nonlocal vdW interaction.

First-principles approaches for how vdW can be treated in DFT were first proposed for the asymptotic interaction between fragments [1–3]. These ultimately evolved into the van der Waals density functional (vdW-DF) for arbitrary geometries [4, 5]. It has been successfully applied to many sparse systems, including the  $\pi$ - $\pi$  stacking interaction [6], organic solids [7–9], molecular adsorption [10–12], layered systems [13], interactions in DNA [14–16], and hydrogen storage in nanoporous materials [17, 18] (See also the review in Ref. 19). Despite its success for describing dispersion in a breadth of systems better than any other nonempirical method [19], vdW-DF underestimates hydrogen-bond strength [20, 21] and overestimates equilibrium separations [4–6, 10, 18, 19, 22, 23]. A recent variant [24] of vdW-DF (denoted vdW-DF-09 by its authors) introduces some empiricism, but has been applied to too few systems to assess usefulness. A more recent functional [25]

has been the subject of further discussion [26, 27].

The revPBE exchange functional [28], which we use with vdW-DF correlation, (i) is generally too repulsive near the equilibrium separation and hence overestimates it [6], and (ii) can bind spuriously by exchange alone, although less so than most other local or semilocal functionals. Other exchange functionals [29, 30] have also been proposed. Performance studies of various exchange functionals for weakly interacting atoms [31] and molecules [32] show the PW86 exchange functional [33], with an enhancement factor proportional to  $s^{2/5}$  at large  $s$ , to give the most consistent agreement with Hartree-Fock (HF) results, without spurious exchange binding and is chosen here. It also is a good match for the vdW-DF2 correlation kernel, although no others were tried. In summary, we recommend that PW86 exchange [32–34] be used with vdW-DF2 correlation, introduced below.

The key to the vdW-DF method is the inclusion of a long range piece of the correlation energy,  $E_c^{nl}[n]$ , a fully nonlocal functional of the density  $n$ . This piece is evaluated using a “plasmon” pole approximation for the inverse dielectric function, which satisfies known conservation laws, limits, sum rules, and invariances [4]. A single parameter model for the pole position was adopted, with the pole residue set by the law of charge-current continuity ( $f$ -sum rule), and the pole position at large wave vector set by the constraint that there be no self-Coulomb interaction. The single parameter is determined locally from electron-gas energy input via gradient corrected LDA [4].

In vdW-DF, the nonlocal piece of the correlation energy is of the form

$$E_c^{nl}[n] = \int d^3r \int d^3r' n(\mathbf{r}) \phi(Rf(\mathbf{r}), Rf(\mathbf{r}')) n(\mathbf{r}'), \quad (1)$$

where  $R=|\mathbf{r} - \mathbf{r}'|$  and  $f(\mathbf{r})$  is a function of  $n(\mathbf{r})$  and its gradient. In fact  $f(\mathbf{r})$  is proportional to the exchange-correlation energy density  $\epsilon_{xc}$  of a gradient corrected LDA at the point  $\mathbf{r}$ . This arose from the imposed requirement that the dielectric function implied by the plasmon

pole model should give an exchange-correlation energy semilocally consistent with a gradient corrected electron gas. We call the semilocal functional that fixes  $f(\mathbf{r})$  in Eq. (1) the *internal functional*.

The above is easier to understand for two separate molecules, although the arguments apply equally well to a pair of high density regions of a sparse composite material. The long range vdW attraction implied by Eq. (1) occurs from the contribution where  $\mathbf{r}$  is on one molecule and  $\mathbf{r}'$  on the other. The definition of  $f(\mathbf{r})$  and  $f(\mathbf{r}')$  varies continuously and independently at each point according to  $\epsilon_{xc}(\mathbf{r})$  and  $\epsilon_{xc}(\mathbf{r}')$ . The quantity  $\epsilon_{xc}$  is taken to consist of a gradient corrected LDA, but what gradient correction should be used? In the first version of vdW-DF for general geometries [4], the gradient correction was obtained from the gradient expansion [35] for the slowly varying electron gas [36, 37]. More appropriate is a functional that gives accurate energies for *molecules*, however. When  $\mathbf{r}$  and  $\mathbf{r}'$  are each in a separate molecule-like region, with exponentially decaying tails between them,  $f(\mathbf{r})$  and  $f(\mathbf{r}')$  can be both large and give key contributions to a vdW attraction. However, for this case (including perhaps even a molecule near a surface) the large- $N$  asymptote [38, 39] and the exchange energy asymptotic series for neutral atoms provide a more accurate approximation. In fact, the exchange parameter [37]  $\beta$  of the B88 exchange functional [40], successfully used in the vast majority of DFT calculations on molecules, can be derived from first principles using the large- $N$  asymptote [41], as can the LDA exchange. It seems obvious, then, that vdW-DF results should be improved if the second order expansion of the exchange in gradients is replaced by the second order large- $N$  expansion. Thus we use the B88 value of  $\beta$  which is 2.222 times larger [37], a value based on agreement between derived [38, 39, 41] and empirical [40] criteria, and the only value tried.

A further problem is what to do about the screening of exchange. In the original gradient expansion [4], this screening term was considerably smaller than the gradient exchange term. We expect that as an estimate, we can without major overall error simply assume that it increases in the same proportion as gradient exchange itself. Therefore we take as a working approximation, that the appropriate gradient coefficient in the “Z” notation [37] will be multiplied by 2.222. Thus one should let  $Z_{ab} \rightarrow 2.222Z_{ab}$  (See Table 1 in Ref. 35). Summarizing: while  $Z_{ab} = -0.8481$  in vdW-DF,  $Z_{ab} = -1.887$  in vdW-DF2, implying changes in the internal functional.

The performance of our new energy functional is assessed via comparisons with quantum chemistry (QC) calculations on the accurate S22 reference dataset [42, 43]. These twenty-two small molecular duplexes for the non-covalent interactions typical in biological molecules include hydrogen-bonded, dispersion-dominated, and mixed duplexes. Binding energies and potential energy curves (PECs) have been recently reported at very ac-

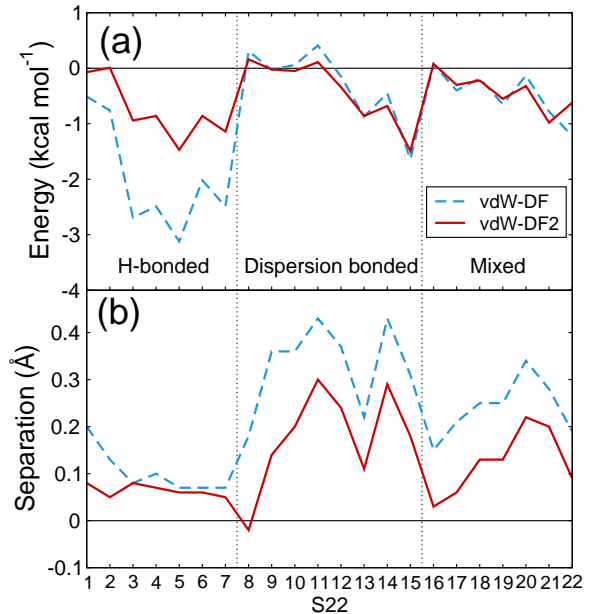


FIG. 1: (Color online) Comparison of (a) binding energies and (b) equilibrium separations for the S22 duplexes. The ordinates give the respective deviations of these quantities from the CCSD(T) values [42]. VdW-DF2 improves the binding energies of hydrogen-bonded duplexes and the separations of vdW-bonded and mixed duplexes.

curate CCSD(T) level with complete basis set (CBS) extrapolation [43]. Recent evaluation [20] of the performance of the vdW-DF for S22 with PBE [44] and revPBE [28] exchange functionals shows it to be quite good, except for H-bonded duplexes, where vdW-DF underestimates the binding energy by about 15%.

Calculations are performed with a plane-wave code and an efficient vdW algorithm [45] with Troullier-Martins type norm-conserving pseudopotentials. Spot comparison with all electron calculations using large basis sets indicates a calculational accuracy of  $\sim 1\%$ , actually better than that of most of PAW potentials supplied in various standard codes. Large box sizes were used to control spurious electrostatic interactions between replicas. See Supplemental Material for further computational details.

For each duplex, a PEC is calculated along the line defined by the center-of-mass coordinates of the molecules, each in its S22 equilibrium geometry of Ref. 42. The orientations of the molecules are kept unchanged. This sampling path and individual molecule geometry exactly matches that of the QC calculation [43], allowing a direct comparison of PECs. Calculated vdW-DF2 binding energies and equilibrium separations, given as a deviation from the S22 geometry along the center-of-mass direction, are compared with the original vdW-DF and the QC calculations in Fig. 1. A typical PEC for each kind of interactions is given in Fig. 2 and details are discussed below. PECs for all the other S22 duplexes are given in

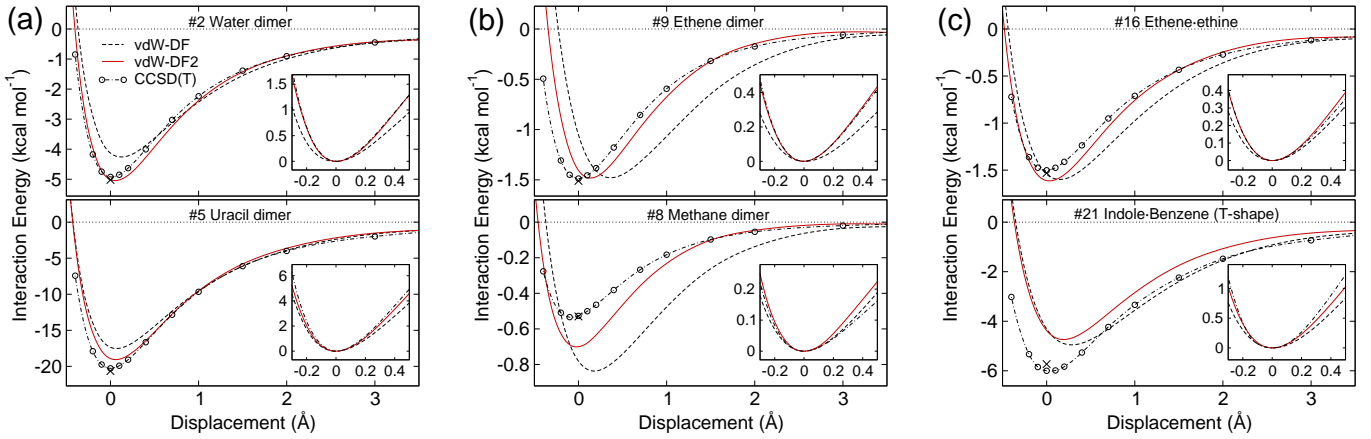


FIG. 2: (Color online) PECs for the best and the worst case of (a) H-bonded (water dimer and uracil dimer), (b) vdW-bonded (ethene dimer and methane dimer), and (c) mixed duplexes (ethene-ethine and indole-benzene). QC PECs (dash-dotted lines with circles) are taken from Ref. 43 and the original S22 reference QC points (cross marks) from Ref. 42. For all the other duplexes, see Supplemental Material.

### Supplemental Material.

Most of the vdW-DF2 binding energies (Fig. 1) are within ‘chemical accuracy’ ( $1 \text{ kcal mol}^{-1}$ ), with a few exceptions (H-bonded uracil dimer, H-bonded A-T pair, and A-T stacked). Mean absolute deviation (MAD) of binding energy is  $0.55 \text{ kcal mol}^{-1}$  (8%), and the MAD of equilibrium separations is  $0.13 \text{ \AA}$  ( $0.95 \text{ kcal mol}^{-1}$ , 13%, and  $0.23 \text{ \AA}$ ). The original vdW-DF values are given in parentheses. Notable improvements are observed in hydrogen-bonded duplexes, where the MADs are  $0.76$  ( $1.95$ )  $\text{kcal mol}^{-1}$  and  $0.06$  ( $0.10$ )  $\text{\AA}$ . The shapes of the PECs near the equilibrium separation are greatly improved, and the strength of the attraction at larger distances is weakened in agreement with QC.

For dispersion-bonded duplexes, the equilibrium separations are much improved (MAD is reduced from  $0.33$  to  $0.19 \text{ \AA}$ ), and binding energies retain quite the same accuracy with vdW-DF (MAD  $0.46 \text{ kcal mol}^{-1}$ ). Another important finding from the comparison of PECs is that vdW-DF overestimates vdW attraction at intermediate range beyond the equilibrium separation, although its minimum energy is accurate. This can contribute to the overestimation of adsorption energy of small gas molecules in nanoporous materials [17, 18]. The vdW-DF2 method shows a very good agreement with QC for all separations, but tends to turn up slightly earlier when approaching the strong repulsion regime at small separations. For duplexes whose large distance asymptote is dominated by dispersion (here methane dimer, ethene dimer, and benzene-methane), vdW-DF2 will have weaker attraction in the asymptotic region and smaller  $C_6$  coefficients than vdW-DF, which (at least for the methane dimer) already gives a  $C_6$  coefficient close to experiment [24]. However, in the region of our calculations, such deterioration is not pervasive. In any case, neither the vdW-DF curves nor the QC curve have

reached their asymptotic limit for any of the above three cases. The remainder of the 22 duplexes have asymptotic forms dominated by electrostatics.

Mixed interaction duplexes share the main features. The equilibrium separations have a MAD equal to  $0.12$  ( $0.24$ )  $\text{\AA}$  and the binding energies have a MAD equal to  $0.44$  ( $0.49$ )  $\text{kcal mol}^{-1}$ . Overall, vdW-DF2 shows the best agreement with QC (except for the indole-benzene duplex), but consistently shows a slightly earlier up-turn when approaching hard-core repulsion regime. This quite universal feature might be due to PW86 exchange functional which is slightly more repulsive than HF at short distances [32].

As a representative model system of important application of vdW-DF to gas storage in organic nanoporous materials, like metal-organic frameworks (MOFs) [18], we calculated  $\text{H}_2$ -benzene duplex and compared with quantum Monte-Carlo (QMC) [46] and MP2/CCSD(T) [47] results. The vdW-DF2 binding energy is not changed, ( $-1.03 \text{ kcal mol}^{-1}$ ), but the separation is decreased by  $0.26 \text{ \AA}$  (from  $3.53$  to  $3.27 \text{ \AA}$ ). The minimum point is in good agreement with recent QMC ( $3.35 \pm 0.079 \text{ \AA}$  and  $-0.96 \pm 0.075 \text{ kcal mol}^{-1}$ ) [46] and MP2/CCSD(T) values ( $3.07 \text{ \AA}$  and  $-0.93 \text{ kcal mol}^{-1}$ ) [47]. However, vdW attraction at intermediate range is much weaker in vdW-DF2 than in vdW-DF. Although there is no QC reference at those separations it is likely that vdW-DF2 is more reliable in this region, because vdW-DF overestimates the binding at intermediate separations for S22 duplexes.

Finally, we tested vdW-DF2 on the internal structure of a water molecule, as an example of strong chemical bonds in molecules. We find that vdW-DF2 does not destroy the accuracy of PBE, which is close to QC and experiment. For details of these tests see Supplemental Material.

In summary, we have presented an enhanced version

of vdW-DF, denoted by vdW-DF2, which can be implemented via simple modifications of existing codes. It results in significant improvements in equilibrium spacings between noncovalently bound complexes, as well as binding energy improvements, especially when hydrogen bonding plays a role. We make a full comparison of PECs of both functionals with accurately known results for a set of 22 complexes, finding favorable results for the new functional. Thus, we expect our method to have important applications in a wide range of fields, ranging from condensed matter and materials physics, chemical physics, and the physics of biological materials.

We thank Valentino Cooper, Andris Gulans, and Risto Nieminen for discussions, Peter Elliott and Kieron Burke for an early copy of Ref. 41, and David Case for the use of his group's computer cluster for several all-electron spot checks. Work supported in part by NSF-DMR-0801343. B. I. L. acknowledges support from the Lundbeck foundation via CAMD.

---

[1] Y. Andersson, D. C. Langreth, and B. I. Lundqvist, *Phys. Rev. Lett.* **76**, 102 (1996).  
[2] J. F. Dobson and B. P. Dinte, *Phys. Rev. Lett.* **76**, 1780 (1996).  
[3] W. Kohn, Y. Meir, and D. E. Makarov, *Phys. Rev. Lett.* **80**, 4153 (1998).  
[4] M. Dion *et al.*, *Phys. Rev. Lett.* **92**, 246401 (2004).  
[5] T. Thonhauser *et al.*, *Phys. Rev. B* **76**, 125112 (2007).  
[6] A. Puzder, M. Dion, and D. C. Langreth, *J. Chem. Phys.* **124**, 164105 (2006).  
[7] J. Kleis, B. I. Lundqvist, D. C. Langreth, and E. Schröder, *Phys. Rev. B* **76**, 100201(R) (2007).  
[8] J. Kleis, E. Schröder, and P. Hyldgaard, *Phys. Rev. B* **77**, 205422 (2008).  
[9] D. Nabok, P. Puschnig, and C. Ambrosch-Draxl, *Phys. Rev. B* **77**, 245316 (2008).  
[10] S. D. Chakarova-Käck, E. Schröder, B. I. Lundqvist, and D. C. Langreth, *Phys. Rev. Lett.* **96**, 146107 (2006).  
[11] P. Sony, P. Puschnig, D. Nabok, and C. Ambrosch-Draxl, *Phys. Rev. Lett.* **99**, 176401 (2007).  
[12] P. G. Moses, J. J. Mortensen, B. I. Lundqvist, and J. K. Nič̄ek, *J. Chem. Phys.* **130**, 104709 (2009).  
[13] E. Ziambaras, J. Kleis, E. Schröder, and P. Hyldgaard, *Phys. Rev. B* **76**, 155425 (2007).  
[14] V. R. Cooper, T. Thonhauser, and D. C. Langreth, *J. Chem. Phys.* **128**, 204102 (2008).  
[15] V. R. Cooper *et al.*, *J. Am. Chem. Soc.* **130**, 1304 (2008).  
[16] S. Li *et al.*, *J. Phys. Chem. B* **113**, 11166 (2009).  
[17] L. Kong *et al.*, *Phys. Rev. B* **79**, 081407(R) (2009).  
[18] L. Kong, G. Román-Pérez, J. M. Soler, and D. C. Langreth, *Phys. Rev. Lett.* **103**, 096103 (2009).  
[19] D. C. Langreth *et al.*, *J. Phys.: Condens. Matter* **21**, 084203 (2009).  
[20] A. Gulans, M. J. Puska, and R. M. Nieminen, *Phys. Rev. B* **79**, 201105(R) (2009).  
[21] A. K. Kelkkanen, B. I. Lundqvist, and J. K. Nič̄ek, *J. Chem. Phys.* **131**, 046102 (2009).  
[22] K. Toyoda *et al.*, *Surf. Sci.* **603**, 2912 (2009).

[23] L. Romaner *et al.*, *New J. Phys.* **11**, 053010 (2009).  
[24] O. A. Vydrov and T. Van Voorhis, *J. Chem. Phys.* **130**, 104105 (2009).  
[25] O. A. Vydrov and T. Van Voorhis, *Phys. Rev. Lett.* **103**, 063004 (2009).  
[26] D. C. Langreth and B. I. Lundqvist, *Phys. Rev. Lett.* **104**, 099303 (2010).  
[27] O. A. Vydrov and T. Van Voorhis, *Phys. Rev. Lett.* **104**, 099304 (2010).  
[28] Y. Zhang and W. Yang, *Phys. Rev. Lett.* **80**, 890 (1998).  
[29] V. R. Cooper, arXiv:0910.1250v1.  
[30] J. Klimes, D. R. Bowler, and A. Michaelides, *J. Phys.: Condens. Matter* **22**, 022201 (2010).  
[31] F. O. Kannemann and A. D. Becke, *J. Chem. Theory Comput.* **5**, 719 (2009).  
[32] E. D. Murray, K. Lee, and D. C. Langreth, *J. Chem. Theor. Comput.* **5**, 2754 (2009).  
[33] J. P. Perdew and Y. Wang, *Phys. Rev. B* **33**, 8800(R) (1986).  
[34] We recommend the refitted version PW86R (see Ref. 32, Table 2) for increased accuracy on the  $\sim 1\%$  level. It was used for the vdW-DF2 calculations here.  
[35] D. C. Langreth and S. H. Vosko, *Adv. Quantum Chem.* **21**, 175 (1990).  
[36] The second order expansion of the vdW interaction, the "c" term in the notation of Ref. 35, was omitted, so that only the "a" and "b" terms are retained, hence the notation  $Z_{ab}$ . See Appendix B of Ref. 5. for a full discussion.  
[37] The relation between  $Z$  and other notations for the gradient coefficient:  $Z = -9\mu = -48\pi(3\pi^2)^{1/3}\beta$ . For pure exchange,  $Z = -10/9$  in the gradient expansion, while for B88,  $Z = -2.469$ .  
[38] J. Schwinger, *Phys. Rev. A* **22**, 1827 (1980).  
[39] J. Schwinger, *Phys. Rev. A* **24**, 2353 (1981).  
[40] A. D. Becke, *Phys. Rev. A* **38**, 3098 (1988).  
[41] P. Elliott and K. Burke, *Canadian J. Chem.* **87**, 1485 (2009).  
[42] P. Jurecka, J. Sponer, J. Cerný, and P. Hobza, *Phys. Chem. Chem. Phys.* **8**, 1985 (2006).  
[43] L. F. Molnar, X. He, B. Wang, and J. Kenneth M. Merz, *J. Chem. Phys.* **131**, 065102 (2009).  
[44] J. P. Perdew, K. Burke, and M. Ernzerhof, *Phys. Rev. Lett.* **77**, 3865 (1996).  
[45] G. Román-Pérez and J.M. Soler, *Phys. Rev. Lett.* **103**, 096102 (2009). We adapted the Siesta [P. Ordejón, E. Artacho and J. M. Soler, *Phys. Rev.* **53**, 10441(R) (1996); J. M. Soler *et al.*, *J. Phys.: Condens. Matt.* **14**, 2745 (2002)] vdW code for use within a private version of Abinit [X. Gonze *et al.*, *Comp. Mat. Sci.* **25**, 478 (2002)]. The vdW interaction was treated fully self-consistently.  
[46] T. D. Beaudet *et al.*, *J. Chem. Phys.* **129**, 164711 (2008).  
[47] O. Hübner, A. Glöss, M. Fichtner, and W. Klopper, *J. Phys. Chem. A* **108**, 3019 (2004).

## Supplemental Material

*Computational details* The convergence control parameters for the plane-wave pseudopotential calculations are tuned until the binding energy is converged up to 0.01 kcal mol<sup>-1</sup>. We used 50 Rydberg kinetic-energy cutoff for hydrocarbon systems and 60 Rydberg for all the oth-

ers containing nitrogen and oxygen. For polar molecules with large dipole moments a  $60 \times 60 \times 60$  Bohr<sup>3</sup> cubic unit cell is needed to eliminate spurious electrostatic interaction between supercell images. The accuracy of the pseudopotentials are tested within PBE [J. Perdew, K. Burke, and M. Ernzerhof, *Phys. Rev. Lett.* **77**, 3865 (1996)] by comparing with all-electron results for the water dimer (duplex #2 in S22) and formic acid dimer (duplex #3). The all-electron energies obtained were also converged to the level of 0.01 kcal mol<sup>-1</sup> (See table I). For water dimer we obtained binding energies (in kcal mol<sup>-1</sup>) of 4.95 (all electron) and 5.05 (pseudopotential). Similarly, for the formic acid dimer we obtained 18.21 (all electron) and 18.40 (pseudopotential). The respective deviations are thus 2% and 1%.

TABLE I: Convergence of all-electron PBE binding energy (kcal mol<sup>-1</sup>) of the water dimer (duplex #2 in S22) and the formic acid dimer (duplex #3). The calculations are performed by Gaussian03.<sup>a</sup> Dunning's correlation consistent basis sets with diffuse functions are used, with counterpoise-corrections.

| basis set   | water dimer | formic acid dimer |
|-------------|-------------|-------------------|
| aug-cc-pVDZ | 4.88        | 17.86             |
| aug-cc-pVTZ | 4.90        | 18.09             |
| aug-cc-pVQZ | 4.94        | 18.21             |
| aug-cc-pV5Z | 4.95        | 18.21             |
| aug-cc-pV6Z | 4.95        | —                 |

<sup>a</sup>Gaussian 03, Revision E.01, M. J. Frisch, G. W. Trucks, H. B. Schlegel, G. E. Scuseria, M. A. Robb, J. R. Cheeseman, J. A. Montgomery, Jr., T. Vreven, K. N. Kudin, J. C. Burant, J. M. Millam, S. S. Iyengar, J. Tomasi, V. Barone, B. Mennucci, M. Cossi, G. Scalmani, N. Rega, G. A. Petersson, H. Nakatsuji, M. Hada, M. Ehara, K. Toyota, R. Fukuda, J. Hasegawa, M. Ishida, T. Nakajima, Y. Honda, O. Kitao, H. Nakai, M. Klene, X. Li, J. E. Knox, H. P. Hratchian, J. B. Cross, V. Bakken, C. Adamo, J. Jaramillo, R. Gomperts, R. E. Stratmann, O. Yazyev, A. J. Austin, R. Cammi, C. Pomelli, J. W. Ochterski, P. Y. Ayala, K. Morokuma, G. A. Voth, P. Salvador, J. J. Dannenberg, V. G. Zakrzewski, S. Dapprich, A. D. Daniels, M. C. Strain, O. Farkas, D. K. Malick, A. D. Rabuck, K. Raghavachari, J. B. Foresman, J. V. Ortiz, Q. Cui, A. G. Baboul, S. Clifford, J. Cioslowski, B. B. Stefanov, G. Liu, A. Liashenko, P. Piskorz, I. Komaromi, R. L. Martin, D. J. Fox, T. Keith, M. A. Al-Laham, C. Y. Peng, A. Nanayakkara, M. Challacombe, P. M. W. Gill, B. Johnson, W. Chen, M. W. Wong, C. Gonzalez, and J. A. Pople, Gaussian, Inc., Wallingford CT, 2004.

TABLE II: Internal structure of a free water molecule. Neither vdW-DF nor vdW-DF2 ruins the accuracy of PBE, and the differences are less than 0.002 Å and 0.5 degree in the OH bond length and the HOH bond angle, respectively. 20×20×20 Bohr<sup>3</sup> cubic unit cell, 130 Rydberg kinetic-energy cutoff, and 0.002 eV/Å force tolerance are used.

| Method               | $d(\text{OH})$ | $\theta(\text{HOH})$ |
|----------------------|----------------|----------------------|
| vdW-DF2              | 0.960          | 105.0                |
| vdW-DF               | 0.960          | 104.7                |
| PBE                  | 0.962          | 104.3                |
| CCSD(T) <sup>a</sup> | 0.958          | 104.5                |
| Expt. <sup>b</sup>   | 0.958          | 104.5                |

<sup>a</sup>D. Feller and K. A. Peterson, *J. Chem. Phys.* **131**, 154306 (2009).

<sup>b</sup>S. V. Shirin *et al.*, *J. Mol. Spectrosc.* **236**, 216 (2006).

TABLE III: Comparison of binding energies and equilibrium separation (displacement along center-of-mass line with respect to S22 geometry) for the S22 duplexes.

| #                             | Duplex                        | Binding energy (kcal mol <sup>-1</sup> ) |         |                 | Displacement (Å) |         |
|-------------------------------|-------------------------------|--|---------|-----------------|------------------|---------|
|                               |                               | vdW-DF                                   | vdW-DF2 | QC <sup>a</sup> | vdW-DF           | vdW-DF2 |
| 1                             | Ammonia dimer                 | 2.66                                     | 3.10    | 3.17            | 0.20             | 0.08    |
| 2                             | Water dimer                   | 4.26                                     | 5.03    | 5.02            | 0.13             | 0.05    |
| 3                             | Formic acid dimer             | 15.92                                    | 17.67   | 18.61           | 0.08             | 0.08    |
| 4                             | Formamide dimer               | 13.54                                    | 15.10   | 15.96           | 0.10             | 0.07    |
| 5                             | Uracil dimer                  | 17.69                                    | 19.18   | 20.65           | 0.07             | 0.06    |
| 6                             | 2-pyridoxine-2-aminopyridine  | 14.74                                    | 15.85   | 16.71           | 0.07             | 0.06    |
| 7                             | Adenine-thymine               | 14.04                                    | 15.23   | 16.37           | 0.07             | 0.05    |
| 8                             | Methane dimer                 | 0.84                                     | 0.69    | 0.53            | 0.18             | -0.02   |
| 9                             | Ethene dimer                  | 1.48                                     | 1.49    | 1.51            | 0.36             | 0.14    |
| 10                            | Benzene-methane               | 1.56                                     | 1.45    | 1.50            | 0.36             | 0.20    |
| 11                            | Benzene dimer (slip-parallel) | 3.14                                     | 2.84    | 2.73            | 0.43             | 0.30    |
| 12                            | Pyrazine dimer                | 4.26                                     | 4.09    | 4.42            | 0.36             | 0.24    |
| 13                            | Uracil dimer (stacked)        | 9.30                                     | 9.26    | 10.12           | 0.22             | 0.11    |
| 14                            | Indole-benzene (stacked)      | 4.75                                     | 4.55    | 5.22            | 0.42             | 0.29    |
| 15                            | Adenine-thymine (stacked)     | 10.64                                    | 10.75   | 12.23           | 0.30             | 0.18    |
| 16                            | Ethene-ethyne                 | 1.60                                     | 1.61    | 1.53            | 0.15             | 0.03    |
| 17                            | Benzene-water                 | 2.85                                     | 2.98    | 3.28            | 0.20             | 0.06    |
| 18                            | Benzene-ammonia               | 2.17                                     | 2.13    | 2.35            | 0.27             | 0.13    |
| 19                            | Benzene-HCN                   | 3.82                                     | 3.91    | 4.46            | 0.24             | 0.13    |
| 20                            | Benzene dimer (T-shape)       | 2.61                                     | 2.42    | 2.74            | 0.34             | 0.22    |
| 21                            | Indole-benzene (T-shape)      | 4.94                                     | 4.75    | 5.73            | 0.28             | 0.20    |
| 22                            | Phenol dimer                  | 5.85                                     | 6.43    | 7.05            | 0.19             | 0.09    |
| Mean deviation (MD)           |                               | -0.87                                    | -0.52   |                 | 0.23             | 0.13    |
| Mean absolute deviation (MAD) |                               | 0.95                                     | 0.55    |                 | 0.23             | 0.13    |
| MAD%                          |                               | 13%                                      | 8%      |                 |                  |         |

<sup>a</sup>P. Jurecka, J. Sponer, J. Cerný, and P. Hobza, *Phys. Chem. Chem. Phys.* **8**, 1985 (2006).

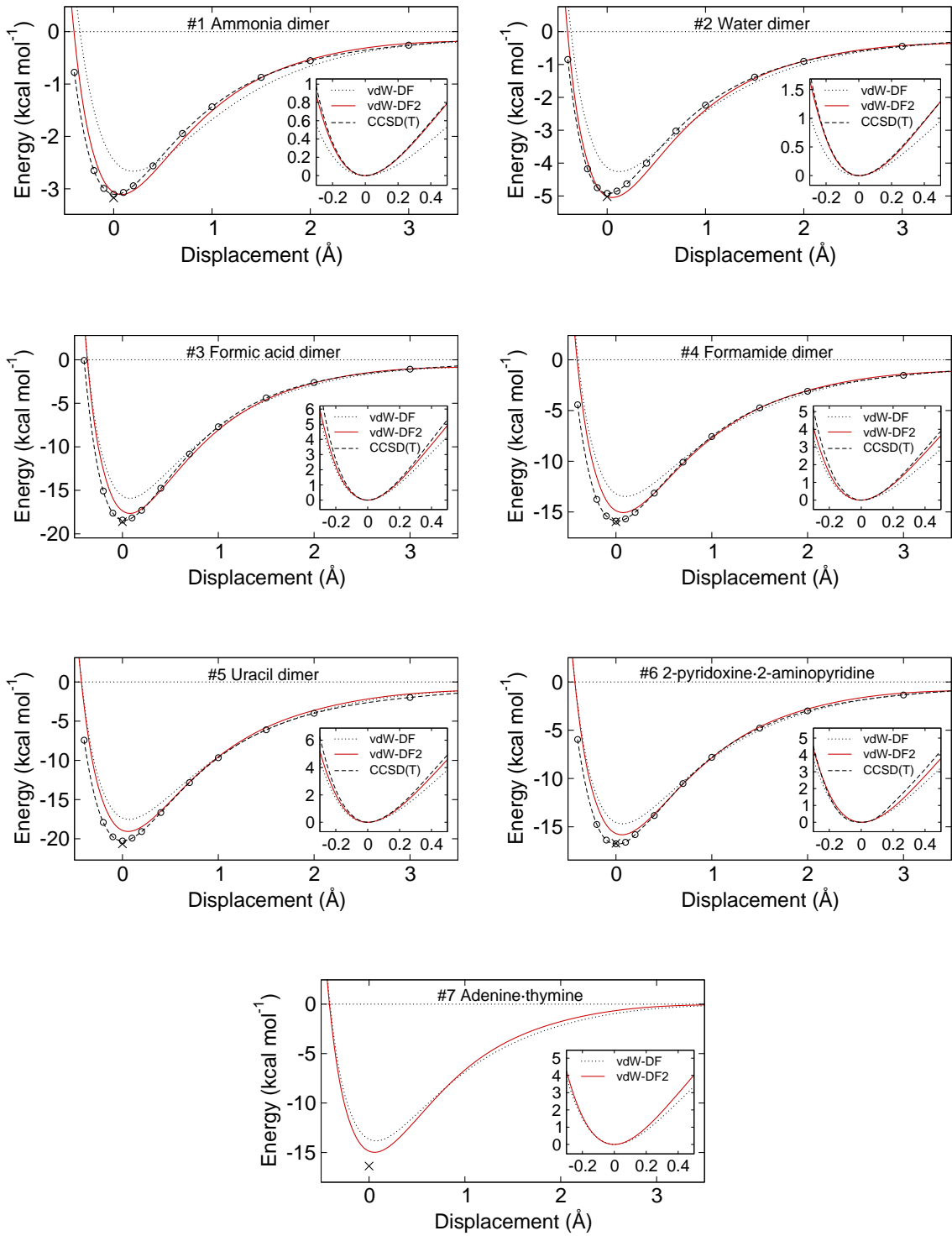


FIG. 3: Interaction energy curves of hydrogen-bonded duplexes. The CCSD(T) data in this and subsequent figures is taken from L. F. Molnar, X. He, B. Wang, and J. Kenneth M. Merz, *J. Chem. Phys.* **131**, 065102 (2009). For the hydrogen-bonded adenine-thymine duplex, CCSD(T)/CBS data are not available.

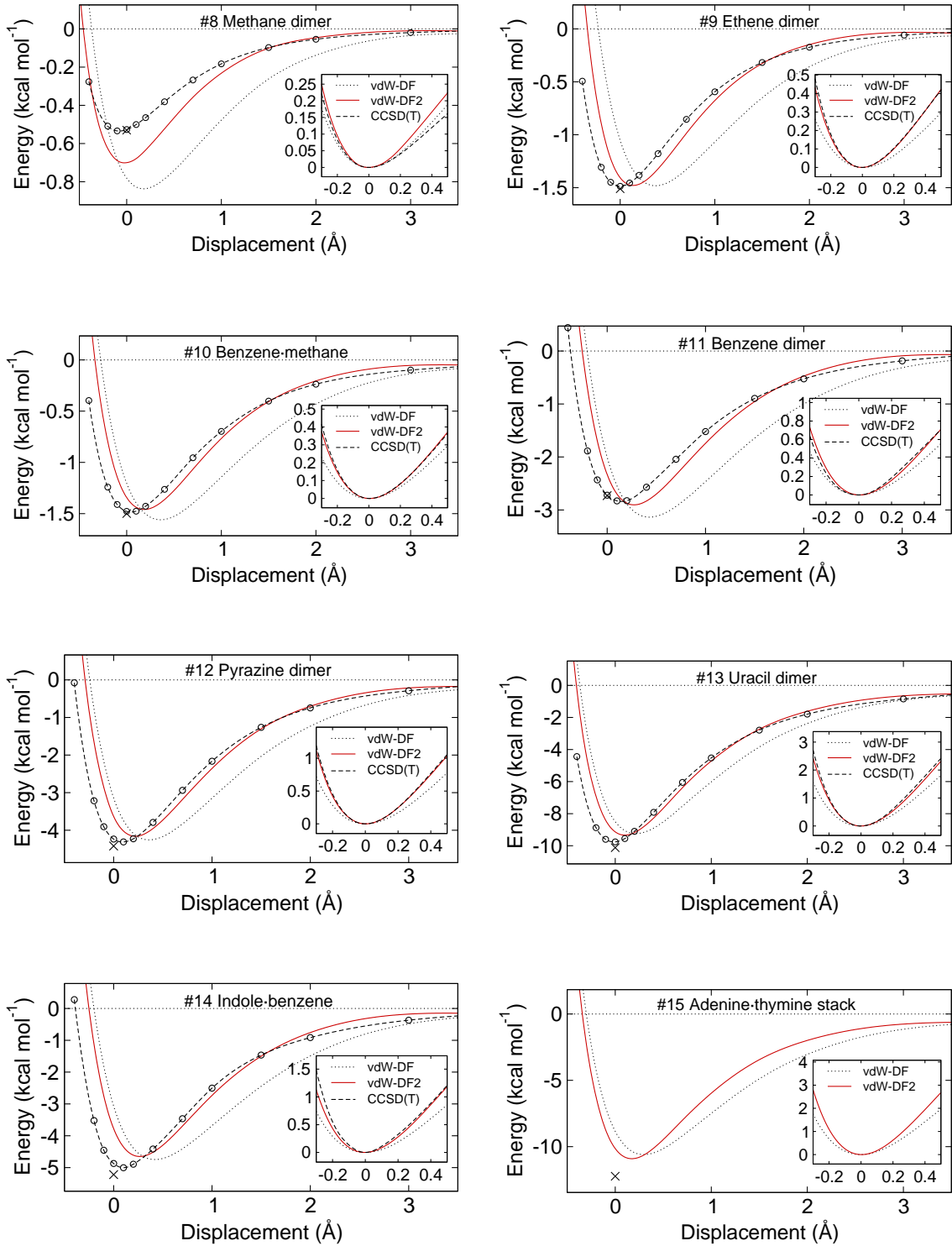


FIG. 4: Interaction energy curves of dispersion-dominated duplexes. For the stacked adenine-thymine duplex, CCSD(T)/CBS data are not available.

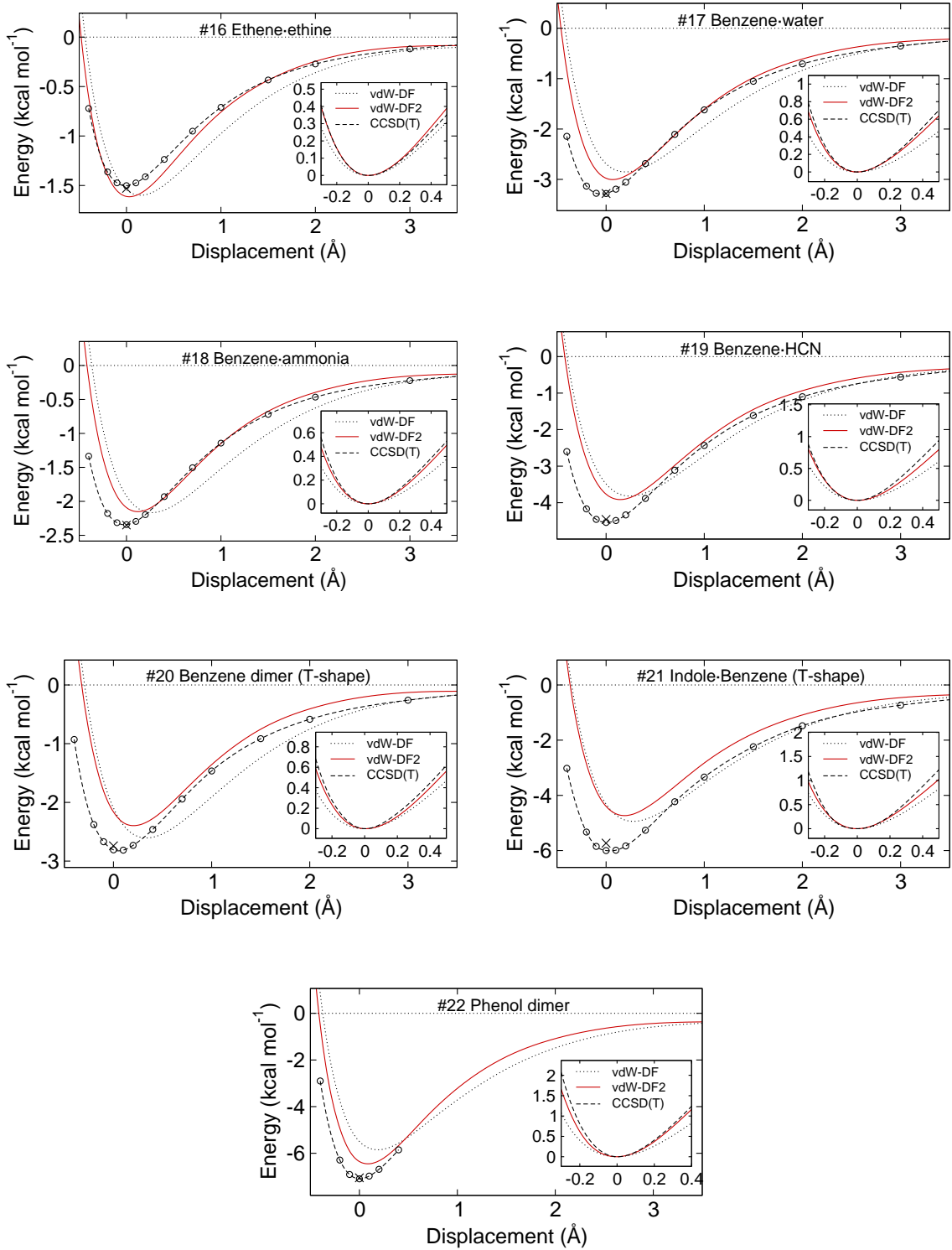


FIG. 5: Interaction energy curves of mixed interaction duplexes.